ISSN 0036-0295, Russian Metallurgy (Metally), Vol. 2018, No. 13, pp. 1222–1228. © Pleiades Publishing, Ltd., 2018.
Original Russian Text © E.M. Visik, E.V. Kolyadov, O.G. Ospennikova, V.V. Gerasimov, E.V. Filonova, 2018, published in Tekhnologiya Metallov, 2018, No. 1, pp. 19–26.

FOUNDRY

Effect of Technological Casting Conditions on the Structure of Single-Crystal Blades Made of a Carbon-Free Nickel Superalloy

E. M. Visik[a], *, E. V. Kolyadov[a], O. G. Ospennikova[a], V. V. Gerasimov[a], and E. V. Filonova[a]

[a] *All-Russia Institute of Aviation Materials (VIAM), Moscow, Russia*

**e-mail: admin@viam.ru*

Received June 25, 2017

Abstract—The process of casting carbonless VZhM4 nickel superalloy cooled blades with a single-crystal ⟨001⟩ structure on UVNK plants is developed. Model blade units with seed parts for the formation of a single-crystal structure in a turbine blade are designed, the structure of the alloy is studied, and experimental batches of single-crystal blade ingots are cast. The influence of the directional solidification conditions on the structure of the carbonless alloy and the susceptibility of the single-crystal structure of the ingots to defect formation are investigated.

Keywords: nickel superalloys, single crystals, liquid-metal coolant, directional solidification, computer designing of alloys

DOI: 10.1134/S0036029518130256

INTRODUCTION

An important advantage of single-crystal turbine blades is their very high thermal fatigue and creep resistance at high temperatures. The creation of the fourth- and fifth-generation nickel superalloys containing rhenium and ruthenium for the high-temperature single-crystal turbine blades of aviation engines in recent years substantially increased their operating temperature and improved their thermal stability.

Foreign alloys EPM-102/MX/PWA1497 (United States) and TMS-196 (Japan) are the most known single-crystal nickel superalloys containing rhenium and ruthenium. The operating temperature of a Russian VZhM4 alloy (FGUP VIAM) is approximately 50°C higher than those of standard ZhS (ZhS26, ZhS32, ZhS36) nickel superalloys used for the turbine blades of a gas turbine engine (GTE) [3–5].

A VZhM4 nickel superalloy (Ni–Al–Mo–Ta–Cr–Co–W–Re–Ru–La system) developed with a computer simulation has no carbon and other grain-boundary hardening elements and is intended for the directional solidification of single-crystal turbine blades, which must have a long service life at elevated temperatures. Table 1 gives the high-temperature strength s of some nickel superalloys intended for casting single-crystal blades with an axial ⟨001⟩ crystallographic orientation (CGO) [6–11].

A necessary condition for casting single-crystal nickel superalloys of the last generation is vacuum-induction melting of a carbon-free VZhM4 alloy (FGUP VIAM) in the form of a rod with a high purity in impurities and gases (mass fractions of O_2, N_2, or S is ≤0.001%) [12].

The technology of casting single-crystal turbine blades made of carbon-containing nickel superalloys (FGUP VIAM) was put into operation for industrial UVNK directional solidification plants with a liquid-metal coolant (aluminum) [13–15]. The technology of casting new single-crystal carbon-free nickel and intermetallic superalloys (VKNA4U, VIN3, VZhM7) for small uncooled turbine blades was developed and tested, and exponential batches of blades were fabricated with a single-crystal structure yield of 80–90% under the industrial conditions of a machine building plant [16, 17].

The most complex problem of casting single-crystal cooled blades made of carbon-free nickel superalloys is the formation of a single-crystal structure over the entire ingot height, especially in the blade platform and foot. For each type of blade, it is necessary to develop a casting unit design with a system of crystal carriers, to adjust casting conditions, and to analyze a structure to increase the ingot-to-product ratio. Various solidification models can be used to predict defects in a single-crystal structure [18, 19].

The purpose of this work is to study the influence of technological casting conditions on the structure of single-crystal cooled turboprop engine blades made of a rhenium-containing ⟨001⟩ VZhM4 superalloy.

Table 1. Long-term strength of single-crystal nickel superalloys

Alloy	Re and Ru content, wt %		$\sigma_{100}/\sigma_{1000}$ (MPa) at temperature		
	Re	Ru	900°C	1000°C	1100°C
ZhS32	4	—	475/330	240/155	120/75
ZhS36	2	—	476/343	250/157	137/83
CMSX-4	3	—	520/360	260/165	140/—
VZhM1	9	—	585/450	330/215	165/95
CMSX-10	6	—	530/400	290/185	150/—
VZhM4	6	4	575/410	305/200	170/120
NC-NG	4	4	475/360	275/190	145/95
EPM-102	5.95	3	503/385	325/200	160/97
TMS-162	4.9	6	565/425	320/230	180/135
TMS-196	6.4	5	590/430	330/—	—/135

EXPERIMENTAL

The conditions of casting blades were adjusted on the directional solidification UVNK-9A plants equipped with an automatic control system in FGUP VIAM and on an industrial UVNK-8P plant. The next-generation UVNK-9A plants have an automatic control system, which increases the reliability of their operation, their capacity due to a decrease in the technological preparation time, and the ingot-to-product ratio. Moreover, in contrast to a commercial UVNK-8P plant, a UVNK-9A plant has a mold heating furnace (MHF), heaters, and thermal shields made of carbon–carbon composite materials, which increases the operating reliability. The vessel with a liquid-metal coolant (Al) is equipped with a vertical motion mechanism to remove the heat gap between heating and cooling zones and to create a temperature gradient at the solidification front (60–80°C/cm) over the entire process of directional solidification.

Single-crystal Ni–W alloy seeds, which were fabricated by orientation cutting with a deviation of $\alpha_{\langle 001\rangle} \le 5°$ from axial CGO, were placed in the seed cavities of ceramic molds for each blade for a single-crystal structure to form in it.

The single-crystal structure of blade ingots after directional solidification was controlled by visual inspection of their surfaces after etching. In contrast to carbon-containing single-crystal alloys, more severe structural requirements are imposed on carbon-free alloy blades: blade ingots must have no grain boundaries because of the absence of carbon and other grain-boundary hardening elements, freckles, spots, equiaxed (recrystallized) grains, and other casting defects. Before heat treatment of the carbonless alloy, any mechanical processing and sand blasting of ingots are avoided to exclude subsequent recrystallization upon heating.

The deviation of the CGOs of blade ingots was determined on starting cones cut from single-crystal ingots, and the plane of cross section was perpendicular to the longitudinal axis of an ingot. The CGO of a single-crystal ingot was determined by X-ray diffraction (XRD) analysis of the cross section of a cone etched to reveal a dendritic structure. X-ray diffraction patterns were recorded with a DRON-3 diffractometer, and angular deviation $\alpha_{\langle 001\rangle}$ of the given axial $\langle 001\rangle$ direction from the longitudinal axis of the cone and, correspondingly, the entire blade ingot was determined. A blade ingot was considered to be good is deviation $\alpha_{\langle 001\rangle}$ did not exceed 10° and the block misorientation was $\Delta\alpha_{\langle 001\rangle} \le 3°$. High-angle boundaries ($\Delta\alpha_{\langle 001\rangle} \ge 3°$) are not allowed in any regions in the blades made of a carbonless alloy.

The microstructures of the polished sections of the blades were analyzed using a JSM-6490LV scanning electron microscope (SEM) and a Leica optical microscope.

RESULTS AND DISCUSSION

The production of single-crystal ingots consists of the nucleation of a single-crystal structure, its motion to the cavity of a mold with starting cavities and crystal carriers, and the growth of a single-crystal structure during directional solidification. A structure nucleates on a single-crystal seed crystal with a given and tested CGO.

The designs of units with starting bases, seed places, and crystal carriers were developed to form turbine blades with a $\langle 001\rangle$ single-crystal structure on a 200-mm-high UVNK-9A plant. The blade model had a starting cone with an angle of ~40°, and its base is a continuation of the blade airfoil profile, which provides the growth of a single-crystal structure into the blade airfoil cavity from the seed placed at the vertex of the cone. To move a single-crystal structure from the starting cone to the foot edges, we placed a crystal carrier in the form of a triangle, the base of which corresponded to its width, from the side of the leading edge and a cylindrical crystal carrier from the side of the trailing edge (Fig. 1a). Model units were assembled from three blades fixed to a pouring basin so that the

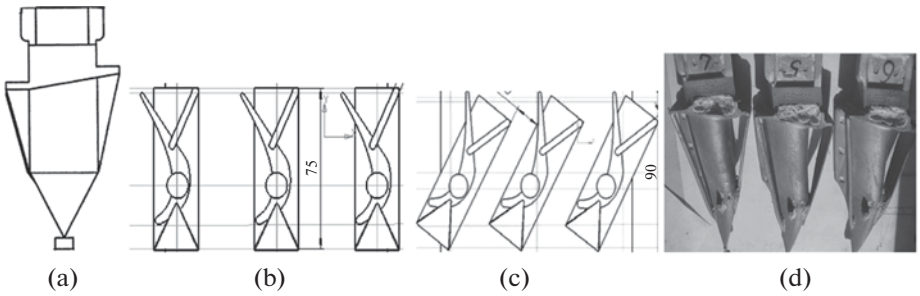

Fig. 1. Sketch of a blade with a starting cone and a crystal carrier system: (a) side view, (b) lateral blade foot surfaces are parallel to heaters, (c) top view of blade units, and (d) single-crystal VZhM4 alloy blade ingots.

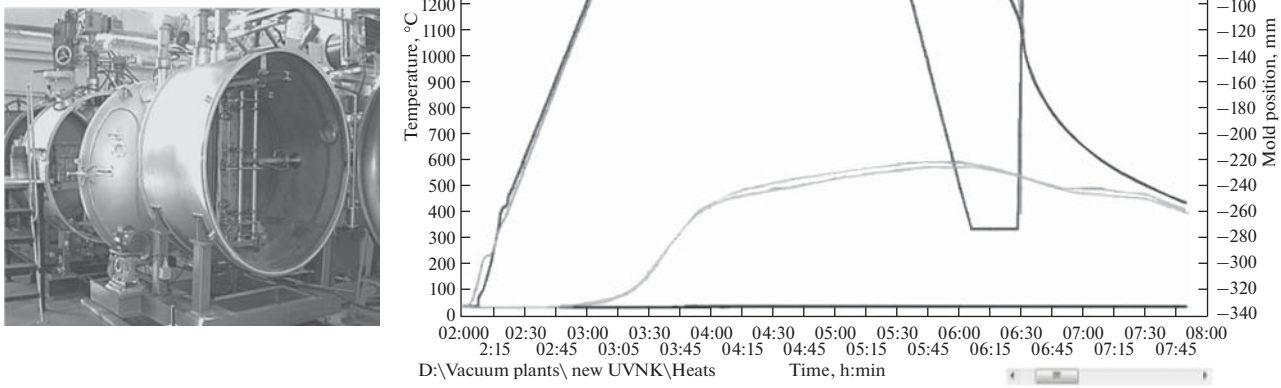

Fig. 2. Appearance of a UVNK-9A plant and the temperature diagram of melting VZhM4 alloy turbine blades.

side platform surfaces were parallel to heaters (Fig. 1b), or blade models were situated so that the side surfaces of the platform surfaces were rotated through an angle of 30°–40° about solidification axis z to the heater plane and the trailing foil edges were parallel to heaters (Fig. 1c).

The process of casting was adjusted on a UVNK-9A directional solidification plant, and an experimental batch of single-crystal VZhM4 alloy blades was cast on a UVNK-8P directional solidification plant under industrial conditions. The temperature casting conditions were identical in both plants: the temperatures were higher than the phase-transition temperatures in the VZhM4 alloy ($T_{solidus}$ = 1370°C, $T_{liquidus}$ = 1450°C) by 150–200°C. A batch of single-crystal blade workpieces was cast on the UVNK-9A plant under the chosen conditions. The velocity of motion of the mold from the heating zone in the liquid-metal coolant (Al) was 6–7 mm/min.

Figure 2 presents the temperature diagram of melting, which shows the temperature distribution in heating, melting, and solidification from the readings of the thermocouples placed at the upper and lower MHF heaters, the induction heater, and the crystallizer (Al). This diagram also demonstrates the path of the mold from the position for casting to the initial zero position (scale is on the right), and stationary thermocouples were used for temperature control (see Fig. 2).

After casting, blade ingots were carefully removed from the ceramic mold, and the pouring basins and the cone starting bases of the single-crystal VZhM4 alloy ingots were cut on a cutting-off machine with cooling and cutting rate control. To avoid recrystallization upon subsequent heating, the ingots were not subjected to sand blasting and chemical etching before homogenization. The results of visual inspection and XRD analysis (with DRON-3 diffractometer) of the etched starting cones of the blade ingots demonstrate

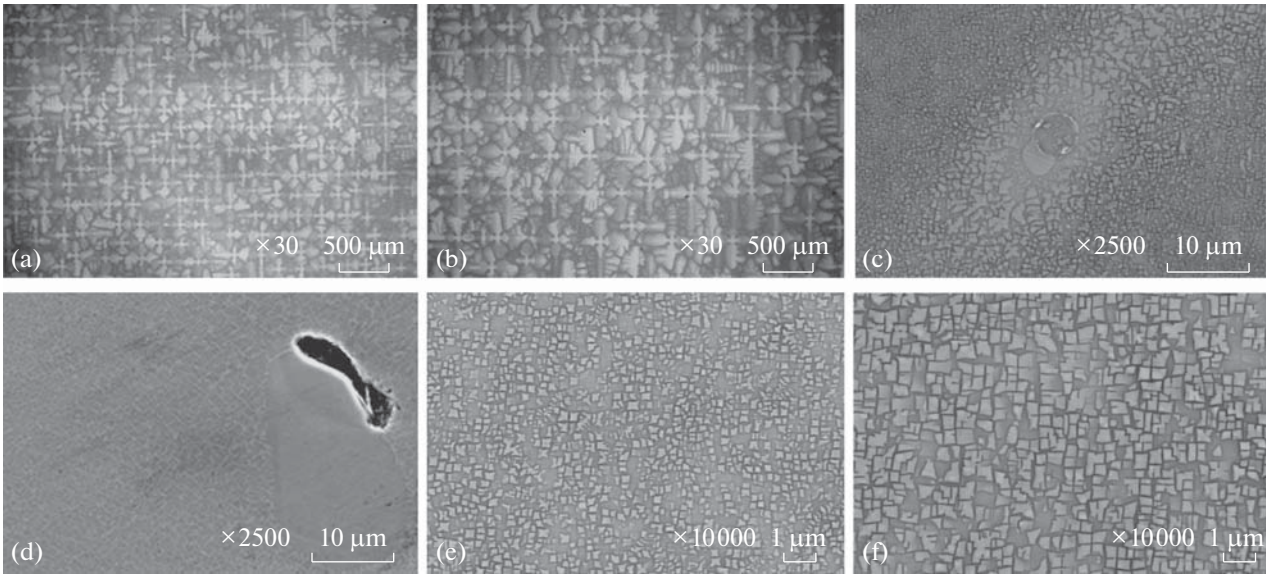

Fig. 3. Microstructure of a single-crystal ⟨001⟩ VZhM4 alloy blade ingot in the as-cast state: (a) cellular–dendritic structure of the blade foil, (b) cellular–dendritic structure of the blade foot, (c) eutectic γ′ phase and casting pores in the interdendritic space, (d) pores in the microstructure of the blade platform, and (e, f) morphology of γ′-phase particles in dendrite arms and the interdendritic space.

that the VZhM4 alloy blade ingots have a ⟨001⟩ single-crystal structure and meet the condition $\alpha_{\langle 001\rangle} \le 10°$.

SEM (JSM-6490LV microscope) studies of the blade alloy in the as-cast state reveal a cellular–dendritic structure with nonequilibrium eutectic γ′-phase precipitates in the interdendritic space, and the size and morphological inhomogeneity of the hardening γ′-phase particles is characteristic of the VZhM4 alloy. Casting pores, the sizes of which correspond to the as-cast state of the alloy, are present in the structure near the eutectic γ′ phase. Low-density regions were not observed in the microstructure of the blade platforms, and casting micropores less than 10 μm in size exist in the structure near the eutectic γ′ phase. Their volume fraction is approximately 0.02%, which corresponds to the as-cast state of a carbonless VZhM4-type superalloy.

All blades were etched after heat treatment (homogenization). When studying the macrostructure of the single-crystal VZhM4 alloy ingots, we detected diffuse boundaries on the platform surfaces of some blades on the side of the trailing edge. After microstructural (optical microscopy) and XRD (DRON-3 diffractometer) investigations of the polished sections cut from the platforms of three blades, we found that these diffuse boundaries are represented by low-angle subgrain boundaries with a small misorientation ($\Delta\alpha_{\langle 001\rangle} \le 3°$) from the main single crystal of the blade with the axial ⟨001⟩ orientation (Fig. 4).

After heat treatment, the low-angle subgrain boundaries usually consist of irregular γ′-phase particles (Fig. 5).

Such low-angle boundaries at the blade foot or platform are allowed in carbonless rhenium-containing superalloy ingots if the CGO of the blade meets the condition $\alpha_{\langle 001\rangle} \le 10°$ and $\Delta\alpha_{\langle 001\rangle} \le 3°$ and corresponds to the blade specifications of a designer. The misorientation of a fragmented structure in blade platforms can be estimated by nondestructive control methods under industrial conditions using special-purpose equipment.

Obviously, the directional heat removal in the foil–platform transition region during solidification changes temporarily, the radial components of the axial temperature gradient are Gx, $Gy > 0$, and secondary dendrite arms grow toward the platform corners. The isoliquidus line becomes concave toward the cooler, which can cause the formation of an isolated supercooled melt region at the platform corners located at long distances; here, heterogeneous nucleation of a crystal, the CGO of which differs from that of the main crystal, is possible at the critical melt supercooling (>20–30°C). Using a heterogeneous nucleation criterion, we can estimate the maximum secondary arm length d_s in a blade platform; this length is determined by growth rate V and time $d_s(t) = \int Vdt$. The time is takes for secondary dendrite arms to grow freely in the lateral direction is $\tau = \Delta T_{cr}/GR$ [20]. Under the given temperature–rate casting conditions,

Fig. 4. Macrostructure of the low-angle subgrain boundaries in VZhM4 alloy blade platforms with various angular misorientation $\Delta\alpha_{\langle 001\rangle}$ (×20).

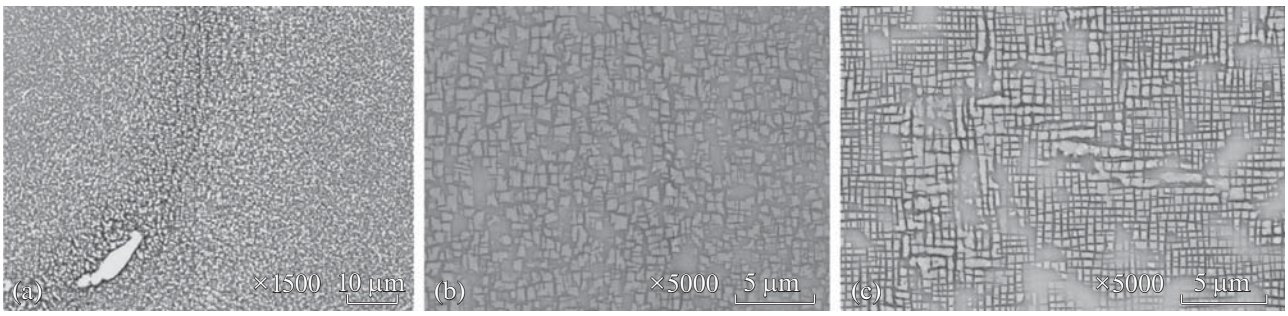

Fig. 5. Microstructure of the low-angle boundaries in VZhM4 alloy blade platforms: (a) in the interdendritic space after casting, (b) after HIP, and (c) after PHT.

the growth of secondary dendrite arms into a blade platform was found to be 20–25 μm, which is a sign of good manufacturability of the VZhM4 alloy. If a crystal carrier from the starting cone is laced at a blade platform corner, no heterogeneous nucleation of foreign crystals takes place; however, structural fragments can appear because of the difference between the dendrite sizes in the main single crystal in the blade and the single crystal of the crystal carrier.

To decrease the probability of appearance of subgrains in a blade platform, we added elements in the form of two gussets adjacent to the cylindrical crystal carrier to the design of the casting unit. In another version, the cylindrical crystal carrier was replaced by a

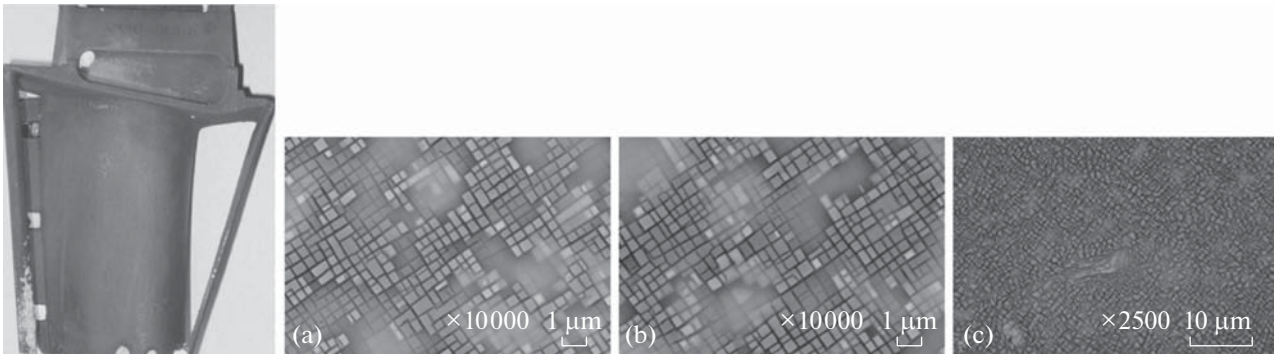

Fig. 6. VZhM4 alloy blade with a single-crystal structure and its microstructure after heat treatment combined with HIP: (a) morphology of γ′-phase particles in dendrite arms, (b) morphology of γ′-phase particles in the interdendritic space, and (c) healed micropore.

triangular plate, which transferred a single-crystal structure from the exit roll to the end face of the plate with smooth transition at the joint. The following technological casting conditions were corrected when blades solidify in the modified casting units in the UVNK-9A and UVNK-8P plants: the solidification rate of the blade unit filled with a metal was decreased from 6 to 4–4.5 mm/min when the solidification front passed through a blade platform, blade platforms were fully submerged in the coolant, and the cooling rate in the upper and lower MHF heaters in the UVNK-8P plant were maintained at a level of 10–20°C/min after the end of motion of the bade units into the coolant to a temperature of 1280 ± 10°C.

This modification of the design of the crystal carriers in the blade unit and the correction of the temperature–rate conditions allowed us to produce cooled VZhM4 superalloy blades with a single-crystal ⟨001⟩ structure without subgrains in a blade foot and platform.

After compete heat treatment combined with HIP, the microstructure of the turbine blade ingots made of a VZhM4 superalloy has no eutectic $\gamma + \gamma'$ precipitates and micropores, and γ'-phase particles have the optimum cuboid morphology characteristic of the VZhM4 alloy (Fig. 6).

CONCLUSIONS

We determined the technological parameters of directional solidification for the production of single-crystal ⟨001⟩ VZhM4 superalloy blades on UVNK-9A plants and under the industrial conditions on a UVNK-8P plant, fabricated an experimental batch of single-crystal ⟨001⟩ turbine blades made of a carbonless VZhM4 superalloy, and improved the design of blade model units to produces blades with a single-crystal structure in a blade foot and platform.

The macro- and microstructures of the blade ingots were studied in the as-cast and heat-treated states. The experimental results can be used to reveal the causes of the appearance of defects in carbonless single-crystal VZhM4 superalloy blades and to increase the ingot yield.

ACKNOWLEDGMENTS

We thank N.V. Petrushin for his management and help.

This work was performed in terms of scientific direction 9.5 Directional Solidification (with Variable Controlled Gradient) of Superalloys (Strategic Trends in the Development of Materials and Technologies of Their Processing up to 2030) [1, 2].

REFERENCES

1. E. N. Kablov, “Innovative solutions of FGUP VIAM GNTs RF for ‘Strategic Directions of Designing Materials and Technologies of Their Processing up to 2030,’” Aviats. Mater. Tekhnol., No. 1, 3–33 (2015). doi 10.18577/2071-9140-2015-0-1-3-33
2. E. N. Kablov, “Strategic trends in the development of materials and technologies of their processing up to 2030,” Aviats. Mater. Tekhnol., No. S, 7–17 (2012).
3. E. N. Kablov, I. L. Svetlov, and N. V. Petrushin, “Nickel high-temperature alloys for casting of blades with directional and single-crystal structure: Part 1,” Materialoved., No. 4, 32–38 (1997).
4. S. Walston, A. Cetel, R. MacKay, K. O’Hara, D. Duhl, and R. Dreshfield, “Joint development of a fourth generation single crystal superalloy,” in *Superalloys 2004* (Minerals, Metals & Materials Society, Pennsylvania, 2004), pp. 15–24.
5. H. Harada, “Development of superalloys for 1700°C ultraefficient gas turbines,” in *Proceedings of 9th Liege Conference on Materials for Advanced Power Engineering 2010* (Belgium: University of Liége, 2010), pp. 604–614.
6. E. N. Kablov, N. V. Petrushin, and I. L. Svetlov, “Computer design of a high-temperature nickel alloy of IV generation for single-crystal gas turbine blades,” in *Cast High-Temperature Alloys. S. T. Kishkin Effect* (Nauka, Moscow, 2006), pp. 98–115.
7. E. N. Kablov, N. V. Petrushin, and E. S. Elyutin, “Single-crystal high-temperature alloys for gas turbine engines,” Vestn. MGTU, Ser. Mashinostroen., No. SP2, 38–52 (2011).
8. E. N. Kablov, O. G. Ospennikova, N. V. Petrushin, and E. M. Visik, “Next-generation single-crystal nickel superalloy with a low density,” Aviats. Mater. Tekhn., No. 2(35), 14–25 (2015). doi 10.18577/2071-9140-2015-0-2-14-25
9. E. N. Kablov, I. L. Svetlov, and N. V. Petrushin, “Ruthenium-containing nickel superalloys,” Aviats. Mater. Tekhn., No. 1, 80–90 (2004).
10. N. V. Petrushin, O. G. Ospennikova, E. M. Visik, L. I. Rassokhina, and O. B. Timofeeva, “Low-density nickel superalloys,” Litein. Proizv., No. 6, 5–11 (2012).
11. N. A. Sharova, E. A. Tikhomirova, A. L. Barabash, A. A. Zhivushkin, and V. E. Brauer, “On the problem of choosing new nickel superalloys for advanced aviation GTE,” Vestn. Samar. Gos. Aerokosm. Univ., No. 3 (19), 249–255 (2009).
12. O. G. Ospennikova, E. M. Visik, V. V. Gerasimov, and E. V. Kolyadov, “Methods for increasing the service properties of gas turbine unit blades,” Tekhn. Metallov, No. 1, 17–24 (2017).
13. E. N. Kablov, *Cast Blades of Gas-Turbine Engines (Alloys, Technologies, and Coatings)* (MISiS, Moscow, 2006).
14. V. V. Gerasimov, N. V. Petrushin, and E. M. Visik, “Improvement of the composition and the development of casting single-crystal blades made of a high-temperature intermetallic alloy,” Trudy VIAM, No. 3,

St. 01 (2015). http://viam-works.ru. Cited April 10, 2017. doi 10.18577/2307-6046-2015-0-3-1-1

15. E. M. Visik, E. A. Tikhomirova, N. V. Petrushin, O. G. Ospennikova, V. V. Gerasimov, and A. A. Zhivushkin, "Technological testing of a new low-density superalloy for casting single-crystal turbine blades," Metallurg, No. 2, 34–40 (2017).
16. E. N. Kablov, V. V. Gerasimov, E. M. Visik, and I. M. Demonis, "Role of directional solidification in the resource-saving technology of production of GTE parts," Trudy VIAM, No. 3, St. 01 (2013). http://viam-works.ru. Cited April 10, 2017.
17. E. M. Visik and V. V. Gerasimov, "Effect of the thermal conditions during directional solidification on the structural parameters of an intermetallic VKNA-4UMono alloy," Metallurg, No. 11, 99–104 (2013).
18. J. D. Miller and T. M. Pollock, "Development and application of optimization protocol for directional solidification: integration fundamental theory, experimentation and modeling tools," in *Superalloys 2012* (Minerals, Metals & Materials Society, 2012), pp. 653–662.
19. J. D. Miller, K. J. Chaput, D. S. Lee, and M. D. Uchic, "Application and validation of directional solidification model dendritic morphology criterion for complex single crystal castings," in *Superalloys 2016* (Minerals, Metals & Materials Society, 2012), pp. 229–236.
20. R. E. Shalin, I. L. Svetlov, E. B. Kachanov, V. N. Toloraia, and O. S. Gavrilin, *Nickel Superalloy Single Crystals* (Mashinostroenie, Moscow, 1997).

Translated by K. Shakhlevich